Observed Atmospheric Response to Cold Season Sea Ice Variability in the Arctic

Claude Frankignoul, Nathalie Sennéchael, Pierre Cauchy

Observed Atmospheric Response to Cold Season Sea Ice Variability in the Arctic

CLAUDE FRANKIGNOUL, NATHALIE SENNÉCHAEL, AND PIERRE CAUCHY

LOCEAN, Université Pierre et Marie Curie, Paris, France

(Manuscript received 2 April 2013, in final form 30 August 2013)

ABSTRACT

The relation between weekly Arctic sea ice concentrations (SICs) from December to April and sea level pressure (SLP) during 1979–2007 is investigated using maximum covariance analysis (MCA). In the North Atlantic sector, the interaction between the North Atlantic Oscillation (NAO) and a SIC seesaw between the Labrador Sea and the Greenland–Barents Sea dominates. The NAO drives the seesaw and in return the seesaw precedes a midwinter/spring NAO-like signal of the opposite polarity but with a strengthened northern lobe, thus acting as a negative feedback, with maximum squared covariance at a lag of 6 weeks. Statistical significance decreases when SLP is considered in the whole Northern Hemisphere but it increases when North Pacific SIC is included in the analysis. The maximum squared covariance then occurs after 8 weeks, resembling a combination of the NAO response to the Atlantic SIC seesaw and the Aleutian–Icelandic low seesaw-like response to in-phase SIC changes in the Bering and Okhotsk Seas, which is found to lag the North Pacific SIC. Adding SST anomalies to the SIC anomalies in the MCA leads to a loss of significance when the MCA is limited to the North Atlantic sector and a slight degradation in the Pacific and hemispheric cases, suggesting that SIC is the driver of the midwinter/spring atmospheric signal. However, North Pacific cold season SST anomalies also precede a NAO/Arctic Oscillation (AO)-like SLP signal after a shorter delay of 3–4 weeks.

1. Introduction

There is increasing evidence that the seasonal to decadal sea ice changes superimposed on the observed decline in Arctic sea ice cover affect the atmospheric circulation. Model studies have suggested that North Atlantic sea ice anomalies influence the North Atlantic Oscillation (NAO)/Arctic Oscillation (AO) and the North Atlantic storm track (Magnusdottir et al. 2004; Alexander et al. 2004; Kvamstø et al. 2004), while North Pacific sea ice primarily influences the atmospheric circulation through the generation of stationary Rossby wave trains (Honda et al. 1999; Alexander et al. 2004; Yamamoto et al. 2006). Deser et al. (2007) showed that the initial adjustment to prescribed North Atlantic sea ice anomalies was a baroclinic response to anomalous surface heat fluxes and changes in low-level baroclinicity in the vicinity of the sea ice changes but that the response became progressively more barotropic and increased in both spatial extend and magnitude owing to transient eddy feedbacks, reaching an equilibrium stage in about 2 months. The transient eddy feedback was linked to Rossby wave breaking by Strong and Magnusdottir (2010). Using monthly observations, Yamamoto et al. (2006) suggested that the dominant interannual mode of midwinter Northern Hemisphere sea ice variability, a seesaw pattern in both Atlantic and Pacific sectors, tends to affect the NAO in late winter via Rossby wave trains triggered by the Pacific sea ice anomalies. Francis et al. (2009) found an association between observed Arctic ice extent in September and the atmospheric circulation in the following autumn and early winter, which seemed to be driven by changes in lower atmosphere stability and cloudiness. Honda et al. (2009) found a link between September ice extent along the Siberian coast and winter climate over Eurasia. Using monthly hemispheric data, Wu and Zhang (2010) found that a reduction of Arctic sea ice concentrations (SICs) in the North Atlantic and the North Pacific sides of the Arctic shelf seas during summer was followed by a negative phase of the NAO/AO during winter.

Since the interannual variability of Arctic SIC, which is mostly associated with the advance or retreat of the ice edge, is primarily driven by main modes of atmospheric variability, feedbacks should be at play. In the North Atlantic the NAO drives the main mode of wintertime

Corresponding author address: Claude Frankignoul, LOCEAN, Université Pierre et Marie Curie, 4 Place Jussieu, 75004 Paris, France. E-mail: cf@locean-ipsl.upmc.fr

DOI: 10.1175/JCLI-D-13-00189.1

SIC variability, a seesaw between the Labrador Sea and the Greenland–Barents Seas, via wind forcing, oceanic heat transport, and surface heat exchanges (Fang and Wallace 1994; Deser et al. 2000). Using Granger causality and weekly time series of the SIC seesaw and the NAO, Strong et al. (2009) showed that the seesaw in the cold season drives a NAO with the opposite phase, thus acting as a negative feedback, in agreement with modeling studies (Magnusdottir et al. 2004; Kvamstø et al. 2004; Deser et al. 2007). However, Wu and Zhang (2010) found that the negative feedback was primarily due to ice in the Greenland–Barents Seas. On the other hand, Yamamoto et al. (2006) suggested that the NAO signal was, in part, damped in response to concomitant ice anomalies in the North Pacific. In the North Pacific the dominant mode of winter sea ice variability exhibits out-of-phase fluctuations between the Bering Sea and the Sea of Okhotsk, which are related to the occurrence of blocking in the Gulf of Alaska and an atmospheric pattern having some similarity with the North Pacific Oscillation (NPO) (Walsh and Johnson 1979; Fang and Wallace 1994). It is significantly correlated with the North Atlantic seesaw (Yamamoto et al. 2006). However, SIC in the two North Pacific areas varies as often in phase (Liu et al. 2007), and the second empirical orthogonal function of wintertime SIC describes the advance or retreat of sea ice in both seas, with greater amplitude in the Bering Sea (Matthewman and Magnusdottir 2011). Linkin and Nigam (2008) found that a positive NPO increases sea ice extent in the Sea of Okhotsk and the western Bering Sea, but Matthewman and Magnusdottir (2011) found that the NPO only influences SIC in the Bering Sea. Using Granger causality between an observed weekly Bering Sea ice index and the NPO, they found that the NPO responds to the Bering SIC changes, acting as a positive feedback. This positive feedback is seen in Wu and Zhang (2010).

In this paper, we further investigate the relation between the Northern Hemisphere atmospheric circulation and SIC changes during the cold season from December to April. The emphasis is on distinguishing the potential influence of North Atlantic and North Pacific SIC variability during the cold season and on assessing whether the concomitant sea surface temperature (SST) anomalies play an active role in the atmospheric changes.

2. Data and method

We use Arctic SIC from the National Snow and Ice Data Center (NSIDC) derived from *Nimbus-7* Scanning Multichannel Microwave Radiometer and Defense Meteorological Satellite Program Special Sensor Microwave Imager radiances (Cavalieri et al. 1996) from 1979 to 2007. The data are available on a 25-km grid every two days for 1978–86 and daily for 1987–2007. As in Strong et al. (2009), we consider weekly means in the 21-week periods starting 5 December and ending about 30 April when the ice extent is large. There is a data gap from 3 December 1987 to 13 January 1988, so the 1987/88 season was omitted. SIC anomalies were obtained by subtracting the 27-yr mean of each week, and grid points with little variations in concentration were excluded: namely, discarding grid points where SIC was larger than 95% or smaller than 5% in at least half of the 27 cold seasons (thus excluding the Kara Sea). It was verified that the results were not sensitive to this precise criteria. Weekly sea level pressure (SLP) anomalies on a Gaussian T62 grid were obtained from the National Centers for Environmental Prediction Climate Forecast System Reanalysis (CFSR) (Saha et al. 2010). For convenience, we also use weekly SST anomaly data from the CFSR since they were strongly damped to the NOAA optimal interpolation $^1/_4°$ daily SST version 2 [Advanced Very High Resolution Radiometer (AVHRR)-only product] (Reynolds et al. 2007). It was verified that the large-scale SST anomaly patterns were nearly indistinguishable between the two products. The SST was considered in ice-free regions on the atmospheric grid, but the results were similar with the original 0.5° resolution. To reduce the influence of trends and low frequency changes, a third-order polynomial was removed by least squares fit from all data. This removes 13% of the SIC anomaly variance and satisfactorily represents the cold season SIC decline of the last decades. Similar results are obtained if a quadratic trend is removed instead.

Lag maximum covariance analysis (MCA) (Bretherton et al. 1992; von Storch and Zwiers 1999) was used to infer cause and effect relationships. The MCA isolates pairs of spatial patterns and their associated time series by performing a singular value decomposition of the covariance matrix between two fields. Each field is expanded into orthogonal patterns that maximize their area-weighted covariance. To establish whether the MCA modes are meaningful, each MCA was repeated at least 100 times, linking the original oceanic anomalies with randomly scrambled atmospheric ones based on blocks of two successive years, as in Czaja and Frankignoul (2002). Note that solely scrambling the field with a short time scale avoids altering the large persistence of the SIC and SST anomalies, which could only be achieved in paired scrambling by using blocks of much longer length. The quoted significance levels indicate the percentage of randomized squared covariance (SC), SC fraction (SCVF), and correlation (R) for the corresponding mode that exceeds the value being tested. These estimates are robust,

changing by a few percent at most between different ensembles of 100 permutations. A smaller significance level indicates stronger evidence against the null hypothesis that there is no relation between atmospheric and oceanic anomalies. Here we primarily discuss the first MCA mode, as it is the only one that suggests a significant SIC impact on the atmosphere.

The atmospheric response to oceanic anomalies can be estimated by MCA for the ocean leading the atmosphere by more than the atmospheric persistence, which should not exceed 10 days (Feldstein 2000), or 2–3 weeks when using weekly data. However, the El Niño–Southern Oscillation (ENSO) introduces a persistent component that could mask the oceanic influence on the atmosphere. Much of the ENSO contamination of the estimated atmospheric response can be removed by linear regression on both oceanic forcing and atmospheric response fields (Frankignoul and Kestenare 2002). When using weekly averages, the ENSO teleconnections cannot be considered instantaneous since they need about a month to affect the extratropical atmosphere (Liu and Alexander 2007). As discussed in the appendix, the teleconnection delay was estimated as 3 weeks, and the removal of the ENSO signal from SIC or SST must be a function of time lag to get an unbiased response. The amount of removed variance may thus depend on the lag. It is small for SLP (2%) and SIC (about 3%), suggesting a weak ENSO impact at the weekly time scale but larger one for SST (17% at lag 0).

The MCA is based on (A6) in the appendix when SLP lags the oceanic variables. Significant modes for the lag exceeding atmospheric persistence are interpreted as an atmospheric response to the oceanic variables. However, it is not excluded that they reflect other concomitant processes that induce low-frequency changes in the atmosphere, such as snow cover variability (e.g., Cohen and Jones 2011) or stratospheric anomalies (e.g., Baldwin and Dunkerton 1999).

3. The influence of sea ice concentration on the atmosphere

a. North Atlantic

The North Atlantic sector is defined between 90°W and 45°E for SLP to represent well the main modes of atmospheric variability and between 90°W and 90°E for SIC, although the domain with substantial SIC variability during the cold season (see criterion in section 2) only covers a smaller area. In this sector, the ice–atmosphere coupling is strongly dominated by a single mode describing the interaction between a SIC seesaw and the NAO. As shown in Fig. 1 (thin line), the squared

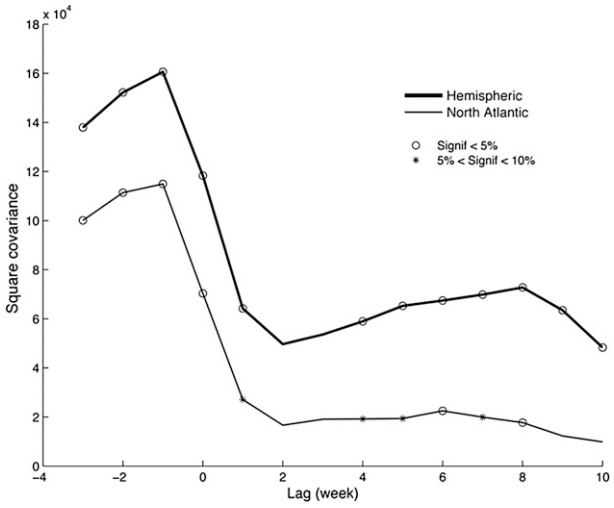

FIG. 1. Squared covariance of the first MCA mode between SIC and SLP as a function of time lag (positive when SIC leads) for the Northern Hemisphere (thick line) and the North Atlantic sector (thin line). Open circles (asterisks) indicate 5% (10%) significance.

covariance of the first MCA mode is maximum when SLP leads SIC by 1–3 weeks. This reflects the fast SIC seesaw response to the NAO variability, with sea ice expansion in the Labrador Sea and retreat in the Greenland–Barents Seas and the northern Baltic following a positive NAO and vice versa for the negative NAO (Figs. 2a,b). This relationship is discussed in Fang and Wallace (1994) and Deser et al. (2000). Consistent with the NAO persistence, the SC decreases but the patterns remain similar when SLP is simultaneous with SIC or follows by 1 week. A transition occurs and significance is lost when SLP lags by 2 weeks, and by 3 weeks SC and significance start increasing slowly with lag. The SC and SCVF are maximum and most significant after 6 weeks and then slowly decrease, losing significance after lag 8. The MCA patterns vary very little with lag, suggesting that the sea ice seesaw drives a positive NAO, albeit with an intensified amplitude at high latitude (Figs. 2c,d). The statistical significance of R is low, however, decreasing with increasing lag (10% at lag 4, 29% at lag 5). We have been unable to explain this behavior. The reversal of SLP polarity suggests that the SIC dipole acts as a negative feedback on the NAO, as found in earlier studies. Since SLP is considered between mid-January and early June when the lag is 6 weeks, the mode is interpreted as a midwinter/spring NAO response to cold season North Atlantic SIC anomalies. Our analysis is in agreement with the modeling study of Magnusdottir et al. (2004). They found that the NAO response was primarily due to SIC in the Greenland–Barents Seas.

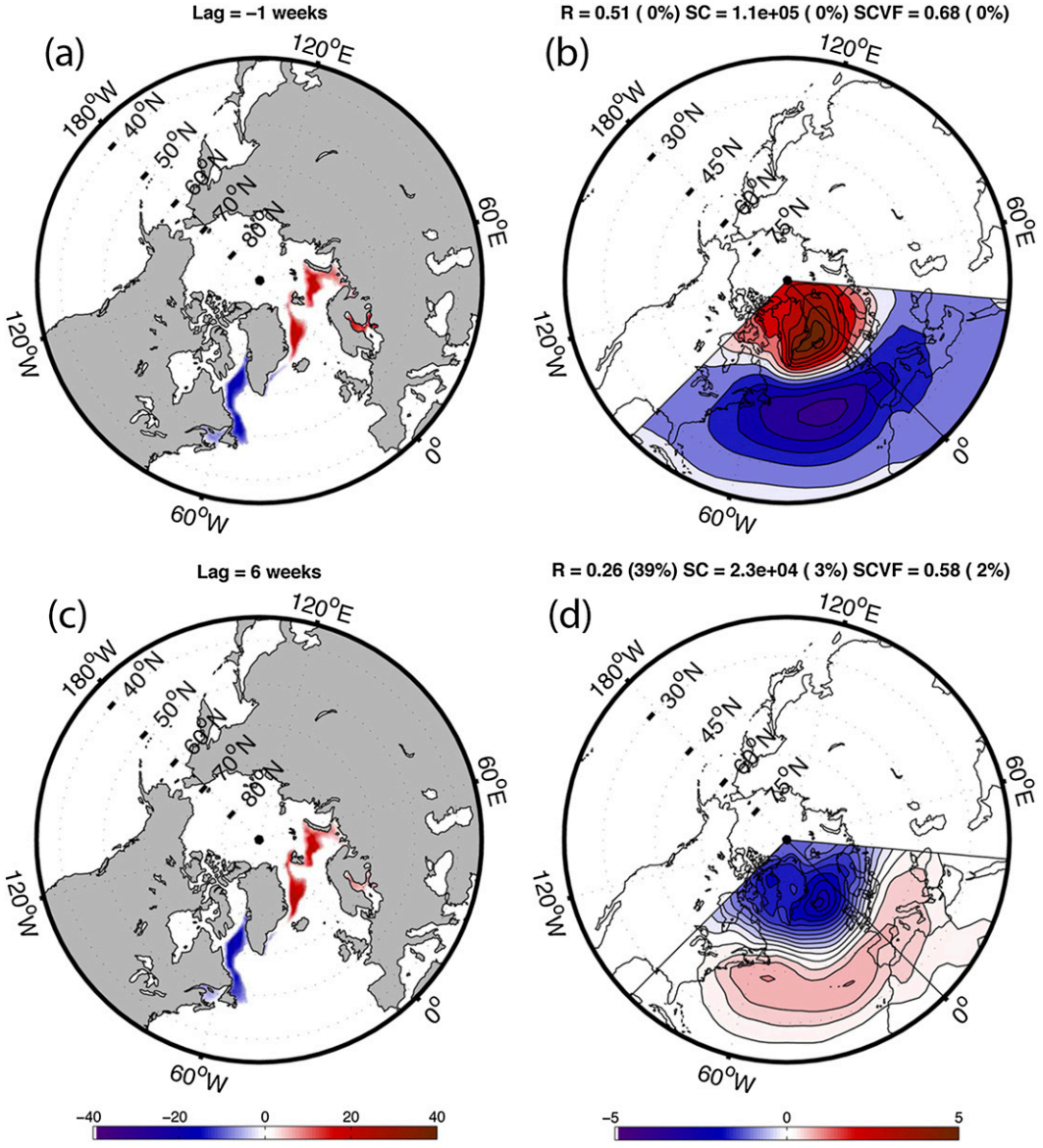

FIG. 2. Covariance map for (left) SIC (%) and (right) SLP (hPa) in the North Atlantic sector when SLP (top) leads SIC by 1 week and (bottom) lags SIC by 6 weeks. The time series were normalized so that the maps show typical amplitudes. The SC, correlation *R*, and SCVF are indicated, with the estimated significance level.

An attempt was made to explore the time dependency of the relation between NAO and SIC by performing the MCA for three overlapping 14-yr periods (years 1–14, 8–21, and 14–27), although the sample is more limited. When SIC lags the atmosphere, the MCA mode shows little change, stressing its robustness. On the other hand, when SIC leads, statistical significance was only found for years 1–14, with patterns as in Figs. 2c,d, although similar MCA patterns were seen for years 8–21 (but not for years 14–27). The bulk of the signal may thus come from the first half of the 1979–2007 period. However, the mode is slightly more significant when the whole period is considered, suggesting that it may also exist during the second half, albeit with a weaker amplitude.

As statistical significance is decreased (14% for SC at lag 5 and 6) when the SLP is extended to the Northern Hemisphere while SIC remains limited to the Atlantic sector, the SIC seesaw impact seems primarily limited to the Atlantic sector. However, another weak SC maximum occurs at a lag of 8 weeks, showing that the seesaw precedes a pronounced high in the North Pacific, a weaker one in the Atlantic, and a low over the polar cap (Figs. 3a,b). This mode appears to reflect the stronger relation found at lag 8 when Pacific SIC is included in the

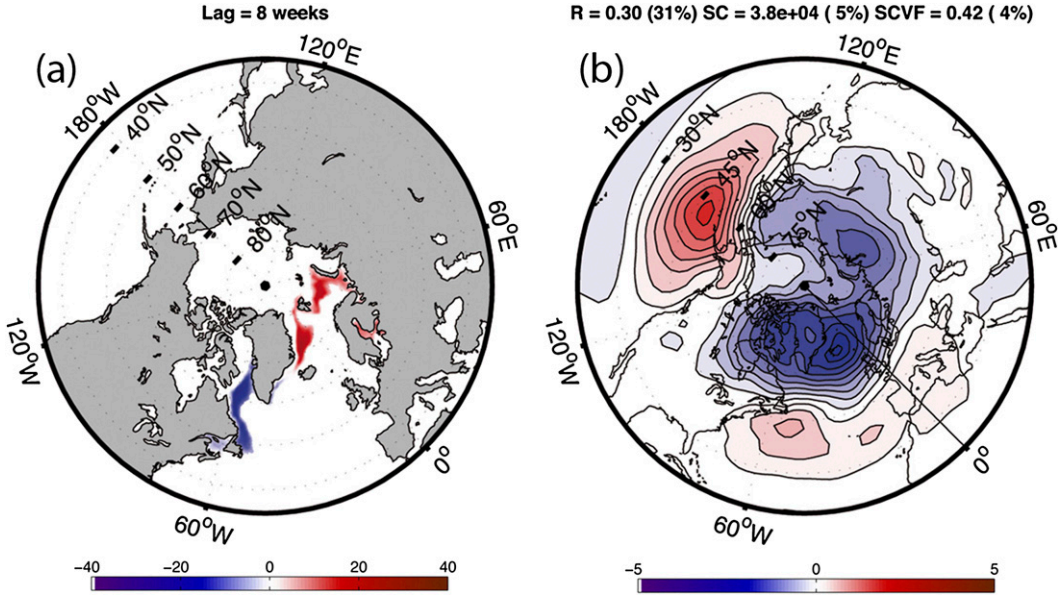

FIG. 3. Covariance map for North Atlantic (left) SIC (%) and (right) hemispheric SLP (hPa) when SLP lags SIC by 8 weeks. The time series were normalized so that the maps show typical amplitudes. The SC, correlation R, and SCVF are indicated, with the estimated significance level.

analysis (see below), hence is unlikely to be primarily driven by the Atlantic SIC changes.

b. North Pacific

In the Pacific sector with SLP taken from 90°E to 90°W, the SC also peaks when SLP leads by 1 or 2 weeks, reflecting the atmospheric forcing of SIC variability. However, the first two MCA modes are poorly separated when SLP leads SIC, and their order change between lag −2 and −1 (mode 1 at lag −1 is essentially mode 2 at lag −2). One mode (mode 1 at lag −2) suggests a pattern somewhat resembling a negative phase of the NPO that decreases the sea ice concentration in the Sea of Okhotsk and western Bering Sea and increases it in the eastern Bering Sea (Figs. 4a,b), not unlike the monthly signals in Linkin and Nigam (2008). The other mode (mode 1 at lag −1) suggests that an east–west SLP dipole drives a slightly different SIC seesaw in the North Pacific (Figs. 4c,d), as in Fang and Wallace (1994). On the other hand, when SLP lags SIC, the first MCA mode is better separated, and it is 5% significant in SC and R between lag 5 and 10 when SLP is taken in the whole Northern Hemisphere, with little change in pattern and maximum SC at the slightly longer lag of 8 weeks, thus for SLP taken from late January to end of spring (Fig. 5, thick line). It shows that a SIC increase in the Sea of Okhotsk and the Bering Sea (Fig. 4e) precedes a SLP pattern resembling a weakening of the Aleutian–Icelandic low seesaw (Fig. 4f), which is particularly apparent in late February and March (Honda et al. 2005). Honda et al. showed that the seesaw is triggered by upper-level Rossby wave trains propagating into the North Atlantic from the Aleutian low in midwinter; hence, the Pacific SIC may indeed influence the NAO by driving a Rossby wave train, as in the response studies (section 1), which could also explain the longer SLP response time. Interestingly, the mode is much less robust when SLP is only taken in the Pacific half of the Northern Hemisphere (from 90°E to 90°W)—it is only 5% significant at lag 8—stressing the hemispheric nature of the SLP signal. Since the modes describing the Pacific SIC response to the atmosphere are not well separated and the SLP patterns differ, feedback is difficult to assess.

The time dependency of the relation with Pacific SIC was explored by performing the MCA in three overlapping 14-yr periods, as in the Atlantic sector. When hemispheric SLP leads SIC, there was little stability in the patterns, as expected from the poor mode separation discussed above. When SIC leads SLP, the covariability was highly significant during years 1–14, with patterns as in Fig. 6. The mode was less significant during years 8–21, with a slightly different pattern in the North Pacific, and it was not found during years 14–27. It is interesting that the SIC influence is largest in both basins during the first half of the period.

c. Hemispheric case

The MCA was then performed with SIC and SLP in the whole Northern Hemisphere (Fig. 1, thick line).

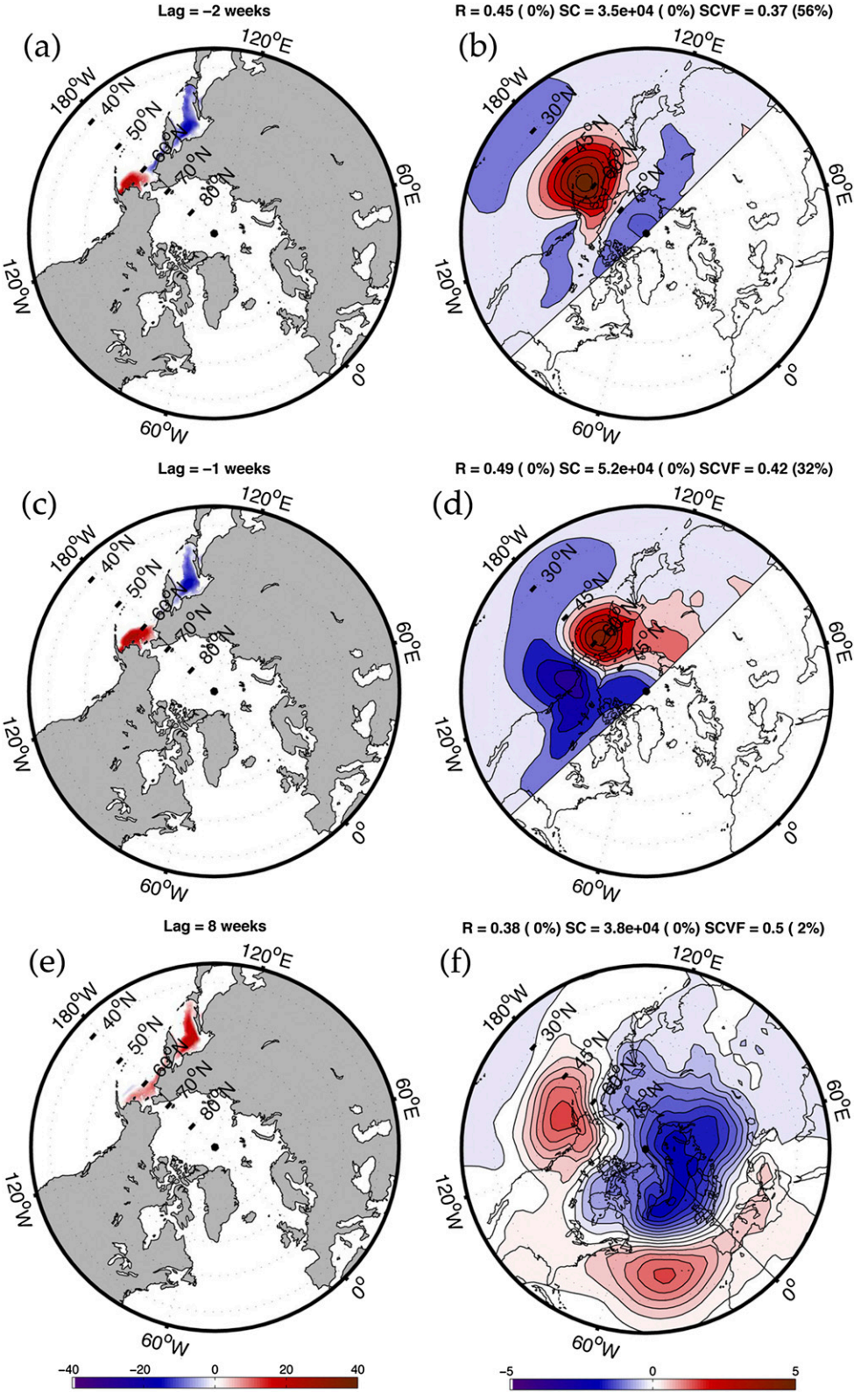

FIG. 4. As in Fig. 2, but in the North Pacific sector when SLP (top) leads SIC by 2 weeks, (middle) leads SIC by 1 week, and (bottom) lags SIC by 8 weeks.

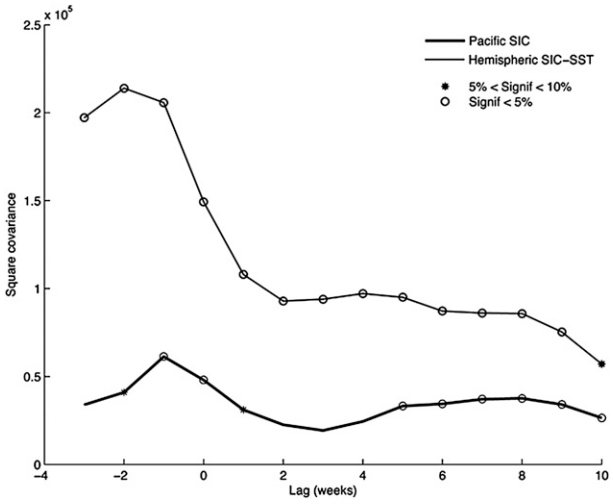

FIG. 5. The SC of the first MCA mode as a function of time lag (positive when SIC leads) between hemispheric SLP and Pacific SIC (thick line) and hemispheric SIC and SST (thin line). Open circles (asterisks) indicate 5% (10%) significance.

When SLP leads SIC by 2 weeks (lag −2), the first MCA mode (which is poorly separated at lag −1) resembles that in Wu and Zhang (2010), showing that a SLP pattern broadly resembling the AO in a negative phase, but for a North Pacific center of action displaced northwestward, drives the SIC seesaw in the Atlantic sector, as in Figs. 2a,b, and an ice retreat in the Bering Sea, with little signal in the Sea of Okhotsk (not shown). When SIC leads SLP, the first MCA mode is better separated and 5% significant in SC, *R*, and SCVF between lag 4 and 9, suggesting a robust atmospheric response. The mode resembles a superposition of the North Atlantic mode in Figs. 2c,d and the Pacific mode in Figs. 4e,f. As in the case where SIC is limited to the Pacific sector, the maximum SC occurs at the lag of 8 weeks, thus for SLP from midwinter to end of spring. The mode (Figs. 6c,d) then resembles the Pacific mode in Figs. 4e,f but for a stronger Pacific high, as in Fig. 3, showing that a SIC increase in the Sea of Okhotsk, the Bering Sea, and the Greenland–Barents Sea precedes an Aleutian–Icelandic low seesaw with an intensified polar lobe. It explains a smaller SCVF (0.43) than when SIC is limited to the Pacific sector (0.5), which suggests that the atmosphere responds to coordinated Pacific and Atlantic SIC forcing but with a predominant Pacific influence. At shorter lag, the SLP pattern has a weaker Pacific high but stronger Atlantic lobes (Figs. 6a,b) so that the Atlantic SIC seesaw may play a more significant role earlier in the season, consistent with the different response time suggested by Figs. 2 and 4. However, the SIC pattern remains similar, so the Atlantic and Pacific influences cannot be disentangled in our short sample. Note that Wu and Zhang (2010) did not detect this late winter/spring mode.

4. Role of the concomitant SST anomalies

Changes in SIC or shifts in the ice edge are accompanied by concomitant SST changes, as the SST is colder where SIC increases and warmer where it retracts. Since the sea ice changes are largely driven by large-scale atmospheric patterns such as the NAO, the SST anomalies also have a large scale. The SST patterns can be obtained by regression onto the SIC time series. However, they do not indicate whether the atmospheric response that we attribute to SIC changes does not simply reflect, or is influenced by, the atmospheric response to the concomitant SST anomalies. To single out the SST influence, we 1) performed corresponding MCAs between weekly SST north of 10°N (similar results were obtained with SST north of 20°N) and SLP anomalies; 2) to assess their role in the lagged relation to SIC, performed MCAs using jointly SST anomalies and SIC anomalies (with SST given equal weight to SIC) as predictor for SLP; and 3) compared statistical significance with MCAs based on SIC alone.

In the North Atlantic sector, no significant MCA mode was found when SST leads SLP, consistent with Czaja and Frankignoul (2002) who only detected a significant North Atlantic SST anomaly influence on the atmospheric circulation in early winter. Correspondingly, adding the SST anomalies to the SIC anomalies in the North Atlantic sector degraded the MCA results obtained with SIC alone, the first mode only reaching a 12% significant SC at lag 6, with a rather noisy SST pattern resembling that obtained by regression on the SIC changes (not shown). This indicates that the North Atlantic SST does not play an active role in the response of the NAO in midwinter/spring to cold season SIC changes. Note that an impact of North Atlantic SST anomalies on the winter NAO has been found in several climate models (Mosedale et al. 2006; Gastineau and Frankignoul 2012), but it occurred later in the season than in the observations (Gastineau et al. 2013).

The results are different in the Pacific sector, as a significant hemispheric SLP signal lags the North Pacific SST in the MCA between SST and SLP. Although the SC and SCVF remain 5% significant until lag 8, the maximum SC is at lag 3 and 4 and the correlation significance strongly decreases at lag ≥5. As shown in Fig. 7, the SST anomaly resembles the Pacific decadal oscillation (PDO), the first North Pacific EOF, and the hemispheric SLP signal broadly resembles the NAO/AO or the warm SST–ridge response with a downstream NAO signal, discussed by Wen et al. (2010), except for

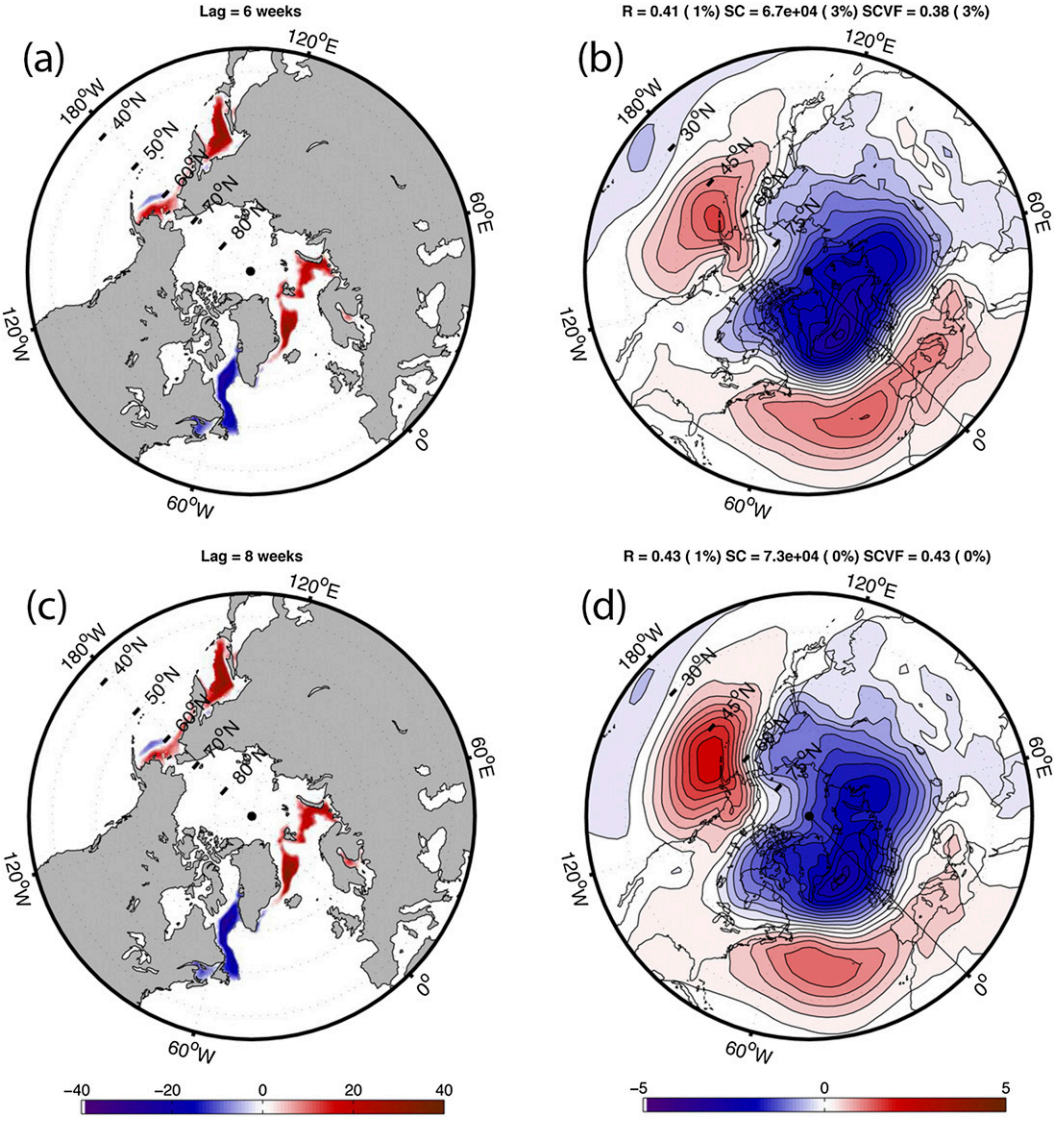

FIG. 6. As in Fig. 2, but for hemispheric (left) SIC (%) leading (right) SLP (hPa) by 8 weeks.

the smaller polar signal in their analysis. Puzzlingly, significance is lost if SLP is limited to the Pacific sector or if Pacific SIC is added in the MCA.

Finally, the hemispheric SST and SIC anomalies were considered jointly in the MCA. Although the SC remains 5% significant when SLP lags by up to 9 weeks (Fig. 5, thin line), significance is lower than with SIC alone, as the first mode is only 5% significant in R at lag 8 (there is a secondary peak in R significance at lag 4). The mode is not well separated (SCVF $\leq$ 0.38), so the patterns should be interpreted with caution. Nonetheless, the mode (Fig. 8) seems to represent a mix of the AO response to North Pacific SST in Fig. 7 and the Aleutian–Icelandic low seesaw response to Northern Hemisphere SIC in Fig. 6. The somewhat different SLP patterns and the slightly stronger SIC anomalies at large lag suggest that SST dominates at lag 3–4 (Figs. 8a–c), while SIC dominates at larger lag (Figs. 8d–f). This would be consistent with the differences in SCVF. Indeed, when hemispheric SLP lags by 4 weeks, the SCVF decreases from 0.53 for North Pacific SST to 0.44 for hemispheric SST, 0.38 for hemispheric SST and SIC, and 0.34 for hemispheric SIC alone. On the other hand, when hemispheric SLP lags by 8 weeks, the SCVF increases from 0.34 for hemispheric SST to 0.38 for hemispheric SST and SIC, 0.43 for hemispheric SIC, and 0.5 for Pacific SIC alone. Similar results are suggested by comparing the SC (after adjustment to have the same oceanic variance): when hemispheric SST is added to hemispheric SIC, the SC increases from 5.9×10^4 to

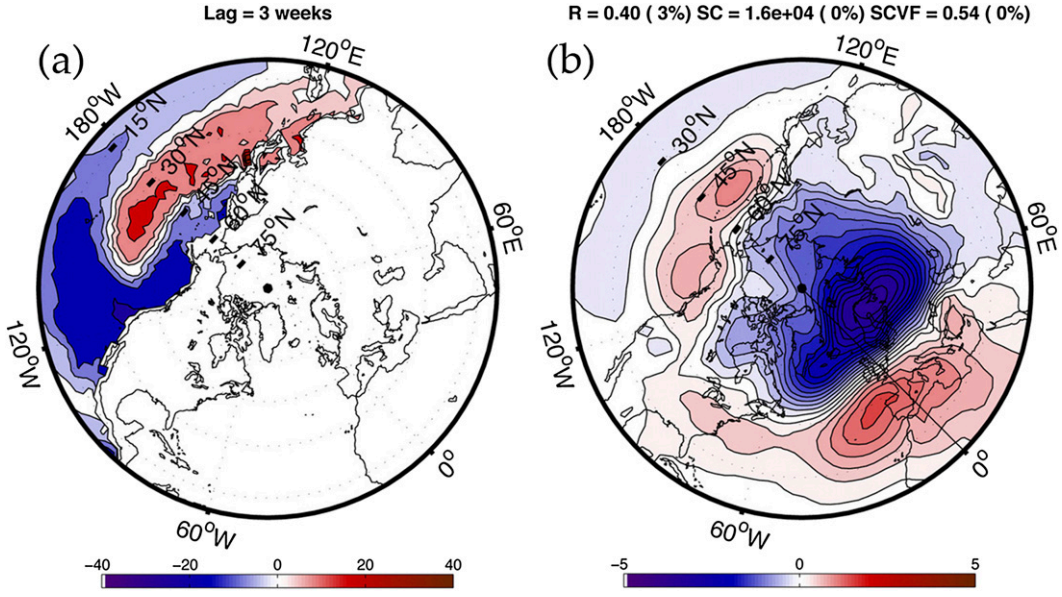

FIG. 7. Covariance map of North Pacific (left) SST (K) and (right) SLP (hPa) when SST leads SLP by 3 weeks. The time series were normalized so that the maps show typical amplitudes. The SC, correlation R, and SCVF are indicated, with the estimated significance level.

6.9×10^4 at lag 4 but decreases from 7.3×10^4 to 6.1×10^4 at lag 8. Note that the North Pacific SST amplitude varies little with lag, presumably because of the larger SST anomaly persistence. In the North Atlantic, the SST pattern is noisy.

5. Discussion and conclusions

The atmosphere–sea ice coupling is strongly dominated in the North Atlantic sector by the interaction between the NAO and a sea ice concentration seesaw between the Labrador Sea and the Greenland–Barents Sea. The NAO drives the seesaw in the cold season and in return the seesaw precedes a weaker, opposite phase of the NAO, albeit with an intensified Icelandic lobe, thus acting as a negative feedback as in the modeling study of Alexander et al. (2004) and the statistical analysis of Strong et al. (2009). However, the latter did not detect the strengthening of the northern lobe of the NAO. Unlike in early winter (Wu and Zhang (2010), both SIC poles seem to contribute to the negative feedback. The signal is most significant at a 6-week lag, broadly consistent with the response time in Deser et al. (2007). The mode seems to describe a midwinter/spring atmospheric response to cold season SIC anomalies. Because of the limited sample, we did not attempt to estimate more precisely the season of maximum signal. Using SLP in the whole hemisphere strongly decreased the statistical significance, while adding the concomitant North Atlantic SST anomalies to the SIC anomalies led to a loss of significance, consistent with the lack of late winter response to North Atlantic SST anomalies (Czaja and Frankignoul 2002). Hence, the SIC seesaw seems to be the driver of the NAO response.

In the North Pacific sector, the first two MCA modes between SIC and SLP are poorly separated when the atmosphere leads. One mode has similarities with the SIC response to the NPO described in Linkin and Nigam (2008), while the other resembles the mode discussed by Fang and Wallace (1994). Hence, the North Pacific SIC response to the atmosphere is not dominated in winter by a single mode, which may explain the inconsistencies in previous North Pacific analyses discussed by Linkin and Nigam (2008). The North Pacific SIC also seems to influence the atmospheric circulation, most significantly when SLP is considered in the whole Northern Hemisphere. An extension of the SIC in the Bering and Okhotsk Seas precedes a SLP pattern resembling the Aleutian–Icelandic low seesaw with maximum covariance and significance at a lag of 8 weeks, thus corresponding to SLP in the late winter/spring period. The signal presumably involves a Rossby wave train propagating in the North Atlantic from the Aleutian low, as in the experiments of Honda et al. (1999), Alexander et al. (2004), and Yamamoto et al. (2006). Although feedback could not be assessed from the MCA in the Pacific case, the patterns are not inconsistent with the positive feedback in the western Bering Sea found by Matthewman and Magnusdottir (2011) and Alexander et al. (2004). When the concomitant Pacific SST anomalies are added to

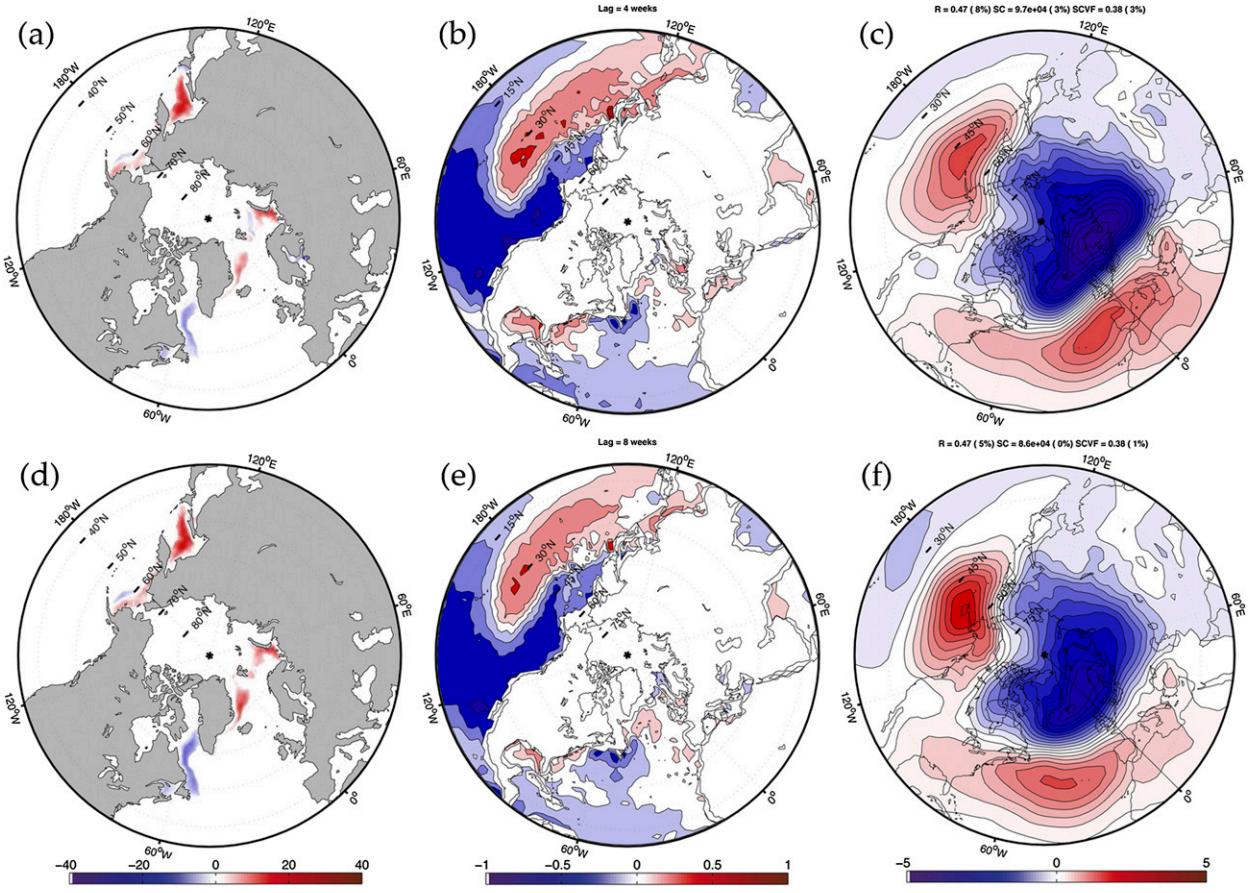

FIG. 8. Covariance map for (left) SIC (%), (center) SST (K), and (right) SLP (hPa) for the first MCA mode between SIC/SST and SLP when SLP lags by (top) 4 and (bottom) 8 weeks. The time series were normalized so that the maps show typical amplitudes. The SC, correlation R, and SCVF are indicated, with the estimated significance level.

the Pacific SIC anomalies in the Pacific sector MCA, significance is lost, while significance is poor at lag 8 with Pacific SST alone. Hence, we conclude that the Aleutian–Icelandic low seesaw response in late winter/spring is primarily driven by SIC. However, PDO-like North Pacific SST anomalies affect the hemispheric circulation at a shorter lag of 3–4 weeks, albeit with a somewhat different response pattern broadly resembling the AO or the warm SST–ridge response with a downstream positive NAO to the first North Pacific SST EOF discussed by Wen et al. (2010). It is noteworthy that Pacific variability seems to be driving SLP on the hemispheric scale while the North Atlantic SIC seems to primarily affect SLP in the North Atlantic sector.

When both SIC and SLP are taken in the whole Northern Hemisphere, the atmospheric signal lagging SIC is quite robust, seemingly combining the atmospheric patterns driven by SIC in the North Atlantic and the North Pacific. Hence, a positive phase of the NAO with an enhanced Icelandic low and a weakening of the Aleutian low—or an Aleutian–Icelandic low seesaw with an intensified polar lobe—follows a sea ice extension in the Greenland–Barents Sea, the Okhotsk Seas, and much of the Bering Sea and a sea ice retreat in the Labrador Sea. Slight changes in the SLP pattern suggest that the Pacific influence is dominant when SIC leads by about 8 weeks and the SC is maximum but that the influence of the Atlantic SIC seesaw increases at shorter lag. Wu and Zhang (2010) found that SIC changes from summer to early winter were influencing the NAO/AO in winter, but they did not detect this late winter/spring response to Northern Hemisphere SIC changes. A longer sample is needed to establish if the hemispheric SLP pattern reflects coordinated SIC forcing in the North Atlantic and the North Pacific, as suggested by Yamamoto et al. (2006), or insufficient separation between Atlantic and Pacific forcing. Since statistical significance, SCVF, and SC are lowered at large lag when the concomitant SST anomalies are added to the SIC anomalies as predictors, SIC seems to be the main driver of the atmospheric response in late winter/spring. However, a more AO-like atmospheric signal was found at shorter lag of 3

and 4 weeks in the MCA using combined SIC and SST anomalies, seemingly reflecting the North Pacific PDO-like SST forcing discussed above, with weaker concomitant SIC anomalies in the North Atlantic. In view of the large SST persistence, the various influences are difficult to disentangle in our short sample.

The time dependency of the relation between cold season SIC and SLP was explored by performing the MCA in three overlapping shorter 14-yr segments. There was no time dependency when the NAO lead the SIC seesaw, but its back interaction on the NAO was only detected during the first half of the 1978–2007 period. Similarly, the Aleutian–Icelandic low seesaw response to Pacific SIC was most clearly identified in the first half of the period and was not identified in the second half. Although in both cases the statistical significance was largest when the full period was considered, there may be some nonstationarity in the SIC–atmospheric coupling.

This study was focused on establishing the statistical links between cold-season sea ice and SST anomalies and the atmosphere in midwinter/spring. They were interpreted as reflecting the atmospheric response to oceanic forcing. The mechanisms controlling the response need to be investigated, and the links with SIC anomalies in the previous summer or early autumn should be clarified, as they impact the atmospheric circulation in winter (Francis et al. 2009; Jaiser et al. 2011) and may provide more extended predictability. In addition, the links with other concomitant processes that may influence the atmosphere, such as snow cover variability (e.g., Cohen and Jones 2011) or stratospheric anomalies (e.g., Baldwin and Dunkerton 1999), should be considered.

Acknowledgments. The research leading to these results has received funding from the European Union 7th Framework Programme (FP7 2007-2013) under Grant Agreement 308299 and the CNRS Programme LEFE/IDAO. We thank C. Strong and an anonymous reviewer for their thoughtful comments and suggestions.

APPENDIX

Removing Delayed ENSO Teleconnections

Some care is required to estimate the observed atmospheric response to extratropical boundary forcing from observations in the presence of delayed ENSO teleconnections. Consider for simplicity the scalar case and assume that the atmospheric response to the oceanic forcing $T(t)$ takes time d to establish and the ENSO teleconnections time c. Then, the atmospheric signal $X(t)$ can be written in a first approximation

$$X(t) = FT(t-d) + bE(t-c) + N(t), \qquad \text{(A1)}$$

where $E(t)$ is the ENSO time series and $N(t)$ the intrinsic atmospheric variability, which is uncorrelated with previous values of T and N at lag larger than its persistence (a week or two at most). As discussed in Frankignoul et al. (2011), the delay d is linked to the (poorly known) time needed for the atmospheric response to reach maximum amplitude. To get unbiased estimates of F, we define a modified atmospheric field

$$\hat{X}(t) = X(t) - AE(t-c), \qquad \text{(A2)}$$

where $A = C_{XE}(c)/C_{EE}(0)$ is obtained by regressing $X(t)$ on $E(t-c)$ and $C_{xy}(\tau)$ denotes the covariance between x and y at lag τ We also define a modified oceanic variable

$$\hat{T}(t) = T(t) - BE(t+d-c), \qquad \text{(A3)}$$

where $B = C_{TE}(c-d)/C_{EE}(0)$ is obtained by regressing $T(t-d)$ on $E(t-c)$. Replacing in (A1) yields

$$\hat{X}(t) = F\hat{T}(t-d) + \left(b + F\frac{C_{TE}(c-d)}{C_{EE}(0)} - \frac{C_{XE}(c)}{C_{EE}(0)}\right)E(t-c) + N(t). \qquad \text{(A4)}$$

Since N and E are uncorrelated, one has by multiplying (A1) by $E(t-c)$,

$$C_{XE}(c) = FC_{TE}(c-d) + bC_{EE}(0). \qquad \text{(A5)}$$

Replacing in (A4) yields

$$\hat{X}(t) = F\hat{T}(t-d) + N(t), \qquad \text{(A6)}$$

which may be used to estimate the atmospheric response when d is larger than the atmospheric persistence. Note that, for each value of the lag d, the ENSO signal must be removed from $T(t)$ by using a regression on $E(t+d-c)$. Hence, for $d = 0$, one uses $E(t-c)$ as in (A2), but for increasing value of d one should use a smaller lag and, for $d > c$, even posterior values of E for the regression on $T(t)$. The method is easily generalized to several ENSO indices.

Here ENSO is defined by the first two principal components (PCs) of weekly SST anomalies in the tropical Pacific between 13°N and 13°S. The teleconnection delay c was defined by the maximum area-weighted variance of the lagged regression of SLP north of 20°N on the ENSO indices in the 25-week period starting 2 January, yielding $c = 3$ weeks. However, the results are not sensitive to the precise value of the delay,

presumably because of the large ENSO persistence. The phase asymmetry of the ENSO teleconnections was taken into account by performing the regression separately for the positive and negative values of the PCs. Note that ENSO removal by linear regression may not fully represent the complex behavior of ENSO teleconnections, but it allows their seasonality and phase asymmetry to be easily represented.

REFERENCES

Alexander, M. A., U. S. Bhatt, J. E. Walsh, M. S. Timlin, J. S. Miller, and J. D. Scott, 2004: The atmospheric response to realistic Arctic sea ice anomalies in an AGCM during winter. *J. Climate,* **17,** 890–905.

Baldwin, M. P., and T. J. Dunkerton, 1999: Propagation of the Arctic Oscillation from the stratosphere to the troposphere. *J. Geophys. Res.,* **104** (D24), 30 937–30 946.

Bretherton, C. S., C. Smith, and J. M. Wallace, 1992: An intercomparison of methods for finding coupled patterns in climate data. *J. Climate,* **5,** 541–560.

Cavalieri, D., C. Parkinson, P. Gloersen, and H. J. Zwally, 1996: Sea ice concentrations from Nimbus-7 SMMR and DMSP SSM/I passive microwave data, 1978–2008. National Snow and Ice Data Center, Boulder, CO, digital media. [Available online at http://nsidc.org/data/nsidc-0051.html.]

Cohen, J., and J. Jones, 2011: A new index for more accurate winter predictions. *Geophys. Res. Lett.,* **38,** L21701, doi:10.1029/2011GL049626.

Czaja, A., and C. Frankignoul, 2002: Observed impact of Atlantic SST anomalies on the North Atlantic Oscillation. *J. Climate,* **15,** 606–623.

Deser, C., J. E. Walsh, and M. S. Timlin, 2000: Arctic sea ice variability in the context of recent atmospheric circulation trends. *J. Climate,* **13,** 617–633.

——, R. A. Tomas, and S. Peng, 2007: The transient atmospheric circulation response to North Atlantic SST and sea ice anomalies. *J. Climate,* **20,** 4751–4767.

Fang, Z., and J. M. Wallace, 1994: Arctic sea ice variability on a timescale of weeks: Its relation to atmospheric forcing. *J. Climate,* **7,** 1897–1913.

Feldstein, S. B., 2000: The timescale, power spectra, and climate noise properties of teleconnection patterns. *J. Climate,* **13,** 4430–4440.

Francis, J. A., W. Chan, D. J. Leathers, J. R. Miller, and D. E. Veron, 2009: Winter Northern Hemisphere weather patterns remember summer Arctic sea-ice extent. *Geophys. Res. Lett.,* **36,** L07503, doi:10.1029/2009GL037274.

Frankignoul, C., and E. Kestenare, 2002: The surface heat flux feedback. Part I: Estimates from observations in the Atlantic and the North Pacific. *Climate Dyn.,* **19,** 633–647.

——, N. Chouaib, and W. Liu, 2011: Estimating the observed atmospheric response to SST anomalies: Maximum covariance analysis, generalized equilibrium feedback assessment, and maximum response estimation. *J. Climate,* **24,** 2523–2539.

Gastineau, G., and C. Frankignoul, 2012: Cold-season atmospheric response to the natural variability of the Atlantic meridional overturning circulation. *Climate Dyn.,* **39,** 37–57.

——, F. D'Andrea, and C. Frankignoul, 2013: Atmospheric response to the North Atlantic Ocean variability on seasonal to decadal time scales. *Climate Dyn.,* **40,** 2311–2330.

Honda, M., K. Yamazaki, H. Nakamura, and K. Takeuchi, 1999: Dynamic and thermodynamic characteristics of atmospheric response to anomalous sea-ice extent in the Sea of Okhotsk. *J. Climate,* **12,** 3347–3358.

——, S. Yamane, and H. Nakamura, 2005: Impacts of the Aleutian–Icelandic low seesaw on surface climate during the twentieth century. *J. Climate,* **18,** 2793–2802.

——, J. Inoue, and S. Yamane, 2009: Influence of low Arctic sea-ice minima on anomalously cold Eurasian winters. *Geophys. Res. Lett.,* **36,** L08707, doi:10.1029/2008GL037079.

Jaiser, R., K. Dethloff, D. Handorf, A. Rinke, and J. Cohen, 2011: Impact of sea ice cover changes on the Northern Hemisphere atmospheric winter circulation. *Tellus,* **64A,** 11595, doi:10.3402/tellusa.v64i0.11595.

Kvamstø, N. G., P. Skeie, and D. B. Stephenson, 2004: Impact of Labrador sea-ice extent on the North Atlantic Oscillation. *Int. J. Climatol.,* **24,** 603–612.

Linkin, M. E., and S. Nigam, 2008: The North Pacific Oscillation–west Pacific teleconnection pattern: Mature-phase structure and winter impacts. *J. Climate,* **21,** 1979–1997.

Liu, J., Z. Zhang, R. M. Horton, C. Wang, and X. Ren, 2007: Variability of North Pacific sea ice and East Asia–North Pacific winter climate. *J. Climate,* **20,** 1991–2001.

Liu, Z., and M. Alexander, 2007: Atmospheric bridge, oceanic tunnel, and global climatic teleconnections. *Rev. Geophys.,* **45,** RG2005, doi:10.1029/2005RG000172.

Magnusdottir, G., C. Deser, and R. Saravanan, 2004: The effects of North Atlantic SST and sea ice anomalies on the winter circulation in CCM3. Part I: Main features and storm track characteristics of the response. *J. Climate,* **17,** 857–876.

Matthewman, N. J., and G. Magnusdottir, 2011: Observed interaction between Pacific sea ice and the western Pacific pattern on intraseasonal time scales. *J. Climate,* **24,** 5031–5042.

Mosedale, T. J., D. B. Stephenson, M. Collins, and T. C. Mills, 2006: Granger causality of coupled climate processes: Ocean feedback on the North Atlantic Oscillation. *J. Climate,* **19,** 1182–1194.

Reynolds, R. W., T. M. Smith, C. Liu, D. B. Chelton, K. S. Casey, and M. G. Schlax, 2007: Daily high-resolution blended analyses for sea surface temperature. *J. Climate,* **20,** 5473–5496.

Saha, S., and Coauthors, 2010: The NCEP Climate Forecast System Reanalysis. *Bull. Amer. Meteor. Soc.,* **91,** 1015–1057.

Strong, C., and G. Magnusdottir, 2010: The role of Rossby wave breaking in shaping the equilibrium atmospheric circulation response to North Atlantic boundary forcing. *J. Climate,* **23,** 1269–1276.

——, ——, and H. Stern, 2009: Observed feedback between winter sea ice and the North Atlantic Oscillation. *J. Climate,* **22,** 6021–6032.

von Storch, H., and F. W. Zwiers, 1999: *Statistical Analysis in Climate Research.* Cambridge University Press, 499 pp.

Walsh, J. E., and C. M. Johnson, 1979: An analysis of Arctic sea ice fluctuations 1953–77. *J. Phys. Oceanogr.,* **9,** 580–591.

Wen, N., Z. Liu, Q. Liu, and C. Frankignoul, 2010: Observed atmospheric responses to global SST variability modes: A unified assessment using GEFA. *J. Climate,* **23,** 1739–1759.

Wu, Q., and X. Zhang, 2010: Observed forcing-feedback processes between Northern Hemisphere atmospheric circulation and Arctic ice coverage. *J. Geophys. Res.,* **115,** D14119, doi:10.1029/2009JD013574.

Yamamoto, K., Y. Tachibana, M. Honda, and J. Ukita, 2006: Intraseasonal relationship between the Northern Hemisphere sea ice variability and the North Atlantic Oscillation. *Geophys. Res. Lett.,* **33,** L14711, doi:10.1029/2006GL026286.